COMPARISON OF THE CONFORMATIONAL STABILITY FOR SEVERAL VINYLHALOMETHANES AND SILANES WITH EXPERIMENT USING MP2 PERTURBATION THEORY AND DFT

Wolfgang FÖRNER[1,*] and Hassan M. BADAWI

Department of Chemistry, King Fahd University of Petroleum and Minerals, Dhahran 31261, Saudi Arabia; e-mail: [1] forner@kfupm.edu.sa

Received September 12, 2006
Accepted November 7, 2006

Dedicated to the memory of the late Professor Jaroslav Koutecký.

In recent literature it was reported that the valence triple zeta basis set augmented by polarization functions is not too reliable for vinyl monohalo- and dihalomethanes and -silanes, the halogen being fluorine and chlorine. The major conclusion was that a valence triple zeta basis is too small to be augmented by polarization functions in a balanced way, at least on vinylmonofluoromethane. Thus we decided to apply the 6-311++G** basis set to the complete series of methanes, silanes and germanes (the latter ones are just added for completeness because no experimental data are available for them and, moreover, we published them already previously) and to compare the results to experimental data available in the literature to see whether the failures of this basis set show up in the complete series of molecules. In the literature we found five such molecules and the information which of the conformers is the most stable. Indeed we found that predictions on the relative stability of conformers in those systems with this basis set and MP2 as well as DFT are with a 60:40 chance, three being correct predictions and two being incorrect ones out of the five. However, since the energy differences are rather small in these systems and due to the fact that – as a consequence of twofold degeneracy of the *gauche* conformer on the potential curve of the torsional vibration – the abundances of the conformers in equilibrium do not change too much, we decided to calculate also vibrational spectra for three examples and to compare them also to experiment. It is reported that besides the failures in total energy (we have chosen two examples where predictions of the nature of the stable conformer are correct, and one where it is not), the vibrational spectra are rather well reproduced, especially when experimental energies are used to calculate abundances in equilibrium in the case where the prediction of the stable conformer failed.

Keywords: MP2; DFT; Conformational equilibria; Theoretical vibrational spectra; Methanes; Silanes; Germanes; Ab initio calculations.

The conformational stability of several vinyl compounds has recently been investigated by density functional (B3LYP) and correlated ab initio calcula-

Collect. Czech. Chem. Commun. 2007, Vol. 72, No. 1, pp. 15–50

doi:10.1135/cccc20070015

tions using a large 6-311++G** basis set to calculate rotational barriers in these molecules[1–4]. The emphasis in this work was on comparisons of the C–M (where M is C, S, P, or As) barriers. Ethenesulfonyl chloride and fluoride $H_2C{=}CHSO_2X$ (X = Cl, F) were found to be predominantly in the *gauche* conformation in which the vinyl group nearly eclipses one of the two S=O bonds[1], yielding conjugation between the coplanar vinyl and S=O groups.

Vinyl ketene $H_2C{=}CH{-}CHCO$ and vinyl isocyanate $H_2C{=}CH{-}NCO$ were found to have a *cis*/*trans* equilibrium with the *trans* form being lower in energy than *cis*[2]. Further it was found that the C–C rotational barrier is considerably higher in energy than the C–N one, due to the difference in the partial π-characters of the C–C and the C–N bond[2].

For vinylphosphonic dichloride and difluoride $H_2C{=}CHP(O)X_2$[3] and vinylarsonic dichloride and difluoride $H_2C{=}CHAs(O)X_2$[4], the planar *cis* forms were found to be about 1.5 kcal/mol lower in energy than the non-planar *gauche* forms. In both molecules the phosponic P=O or the arsonic As=O bond in the predominant *cis* conformation was again predicted to eclipse the vinyl group[3,4]. The *cis–gauche* barrier for the internal rotation around the C–As bond was calculated to be of the order of about 2.5 kcal/mol, which is less by about 0.5 kcal/mol than that calculated for the vinylphosphonic dihalides $H_2C{=}CHP(O)X_2$[3]. The decrease in the rotational barrier as going from vinylphosphonic dihalides to vinylarsonic dihalides was explained as being due to decrease in the covalent bond characters when going from the C–P to the C–As bond. The relative stability of the low-energy conformers in all the vinyl compounds mentioned above could be explained as a result of a noticeable conjugation between the vinyl and the substituent groups[1–4].

Our calculations were performed, using the Gaussian98 program[5] running on an IBM RS/6000 43P model 260 workstation. We carried out DFT-B3LYP/6-311++G** and ab initio MP2/6-311++G** calculations. On DFT and MP2 levels, the geometries of our molecules were fully optimized. The calculations were done for the complete series of vinylmonohalo- and dihalomethanes and -silanes with fluorine and chlorine as the halogens. Of our previously published results[6] we added, for the sake of comparison, the corresponding germanes, for which no experimental data are published in the literature.

In addition we calculated, for comparison, the vibrational infrared and Raman spectra of some of the molecules where experimental spectra are published, using the computational methods previously described[7–10]. We have chosen two examples where we get approximately correct relative energies for the conformers, i.e. vinyldifluoromethane and vinyldifluoro-

silane. Another example is that where the *cis* conformer is experimentally the stable one[11], while in our calculations *gauche* turned out to be more stable, i.e. vinyldichlorosilane. We have seen previously[8,12,13] that the spectra calculated in this way are in reasonable agreement with experimental ones, provided that the abundances in the conformational equilibria are calculated from experimental relative energies. In that case we used both abundances, one set calculated with theoretical Gibbs energies, the other one with experimental relative energies, although the differences between the two sets are not very pronounced because of the twofold degeneracy of the *gauche* conformer on the potential curve.

Our interest in this study resulted from the finding reported by Galabov et al.[14] that in 3-fluoropropene diffuse functions together with a relatively small basis set (like in 6-311++G**) should increase the stability of the *gauche* form to an unreasonable extent. We were basically interested in finding out whether this effect occurs not only for 3-fluoropropene, but also for the higher silane homologues and for fluoro and chloro derivatives. The results of the corresponding germanes published earlier[6] are included in our table for the sake of completeness.

Initially, however, the interesting structures of organosilanes[15–21] and organogermanes[22–31] had attracted our attention to investigate the conformational and structural stability of vinylmonochlorogermane (H_2C=CH–GeH_2Cl) and vinyldichlorogermane (H_2C=CH–$GeHCl_2$), a study which had been published in ref.[6].

Ab initio CALCULATIONS

The structures of our molecules (Fig. 1) were optimized by minimizing the energy with respect to all the geometrical parameters at DFT and MP2 level of calculation.

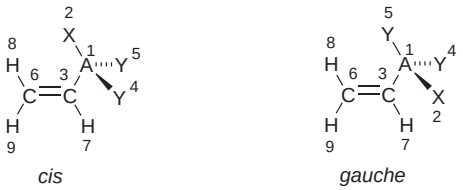

FIG. 1
Common atom numbering in the series of compounds, H_2C=CH–AXY_2, where A is C for the methanes, Si for the silanes, and Ge for the germanes, while in the monohalo derivatives X is a halogen, and Y is H while in the dihalo derivatives X is H and Y is a halogen

The calculated structural parameters, rotational constants and total dipole moments of the stable conformers of the molecules are actually not listed in tables, simply because too large a collection of numbers would result; furthermore, for such geometrical parameters for most of our molecules no experimental data are available. Actually, there are no pronounced differences between the two levels of calculation, and thus we performed the following spectra calculations on DFT level. All molecules exist in a conformational equilibrium between the stable *cis* and *gauche* conformers. In all molecules the *trans* form is a transition state of the internal rotation. In the monohalo derivatives the *gauche* forms are slightly more stable than the *cis* conformers, while in the dihalo derivatives usually *cis* is more stable than *gauche*. This does not change upon adding the zero-point vibrational contribution to the total energy. However, it is pointed out in[14] that the stabilization of *gauche* forms is an artifact of our basis set.

Calculation of Vibrational Spectra

Vibrational spectra can be calculated and plotted from the Gaussian98 output. The general formalism for this procedure can be found in Appendix. As mentioned, for equilibrium mixtures abundances or populations must be calculated. This is best based on equilibrium constants and thus finally on the Gibbs energies for the conformers at 298.15 K and 1 atm pressure. Thus populations of, say, N conformers in equilibrium (in our cases two of them) are calculated from the Gibbs energies at 298.15 K, provided by the program.

If N conformers, C_j, j = 1 to N, are linked by a sequence of $N - 1$ coupled equilibria

$$C_j \leftrightarrow C_{j+1}, \quad j = 1, N - 1 \tag{1}$$

with equilibrium constants, K_i^o

$$K_i^o = \frac{[C_{i+1}]}{[C_i]}, \quad i = 1 \text{ to } N - 1 \tag{2}$$

where square brackets denote concentrations, and if G_i^o is the standard Gibbs energy of conformer i, then for the equilibrium linking C_i with C_{i+1} we have the Gibbs energy change

$$\Delta G_i^o = G_{i+1}^o - G_i^o; \quad i = 1 \text{ to } N - 1 . \tag{3}$$

Thus K_i^o is given by

$$K_i^o = \frac{g_{i+1}}{g_i} \, e^{-\frac{\Delta G_i^o}{RT}} \tag{4}$$

where g_i is the symmetry number of conformer *i*, being 1 when no rotor involved is in the *gauche* position, and in general 2 when one or more rotor is in the *gauche* position. Then, with $K_0^o = 1$, we have

$$[C_i] = [C_1] \prod_{j=0}^{i-1} K_j^o \; ; \; i = 1 \text{ to } N \tag{5}$$

and

$$\sum_{l=1}^{N} [C_l] = [C_1] \sum_{l=1}^{N} \prod_{j=0}^{i-1} K_j^o \; . \tag{6}$$

The abundance, P_i, of conformer *i* in the complete conformational equilibrium is then given by

$$P_i = \frac{[C_i]}{\sum_{l=1}^{N} [C_l]} \; ; \; i = 1 \text{ to } N \tag{7}$$

and thus finally

$$P_i = \frac{\prod_{j=0}^{i-1} K_j^o}{\sum_{l=1}^{N} \prod_{j=0}^{i-1} K_j^o} \; ; \; i = 1 \text{ to } N \tag{8}$$

with $K_0^o = 1$ (it is actually arbitrary, because it cancels anyway).

This equation looks rather unpleasant, but it can be simplified, by taking into account that the product of two equilibrium constants, K_i^o and K_{i+1}^o, of the equilibria coupled by the conformer C_{i+1} is rather simple. Since

$$\begin{aligned} \Delta G_i^o &= G_{i+1}^o - G_i^o \\ \Delta G_{i+1}^o &= G_{i+2}^o - G_{i+1}^o \end{aligned} \tag{9}$$

the product simplifies to

$$K_i^o K_{i+1}^o = \frac{g_{i+1}}{g_i} \frac{g_{i+2}}{g_{i+1}} \, e^{-\frac{\Delta G_i^o + \Delta G_{i+1}^o}{RT}} \tag{10}$$

which reduces to

$$K_i^{\circ} K_{i+1}^{\circ} = \frac{g_{i+2}}{g_i} \mathrm{e}^{-\frac{G_{i+1}^{\circ} - G_i^{\circ} + G_{i+2}^{\circ} - G_{i+1}^{\circ}}{RT}} \tag{11}$$

and thus the influence of C_{i+1} cancels out

$$K_i^{\circ} K_{i+1}^{\circ} = \frac{g_{i+2}}{g_i} \mathrm{e}^{-\frac{G_{i+2}^{\circ} - G_i^{\circ}}{RT}} . \tag{12}$$

Therefore in each sequence of products all intermediate conformers cancel out and only the last one and the first one remain in the populations

$$P_i = \frac{S(i)\, \mathrm{e}^{-\frac{\Delta_i G^{\circ}}{RT}}}{\sum_{j=1}^{N} S(j)\, \mathrm{e}^{-\frac{\Delta_j G^{\circ}}{RT}}} \tag{13}$$

with $S(i) = g_i/g_1$ and $\Delta_i G^{\circ} = G_i^{\circ} - G_1^{\circ}$. Since S is as a factor at every term in the nominator and in the denominator, $1/g_1$ cancels, yielding finally

$$P_i = \frac{g_i\, \mathrm{e}^{-\frac{\Delta_i G^{\circ}}{RT}}}{\sum_{j=1}^{N} g_j\, \mathrm{e}^{-\frac{\Delta_j G^{\circ}}{RT}}} . \tag{14}$$

The order of conformers is completely arbitrary, but the most convenient one will be the order of decreasing stability of the conformers, with the most stable one being C_1.

A crude first estimate of the equilibrium constant, K, at 298.15 K for the *gauche*↔*cis* equilibrium could be the ratio of the two populations P_{cis}/P_{gauche} (as used previously by us), which is

$$K = \frac{P_{cis}}{P_{gauche}} = \frac{g_{cis}}{g_{gauche}} \mathrm{e}^{-\frac{\Delta E}{RT}} ; \quad \Delta E = E_{cis} - E_{gauche} \tag{15}$$

where $g_{cis}/g_{gauche} = 0.5$ is the ratio of the symmetry numbers of the two conformers, R denotes the gas constant, and the E-s are the total energies of the conformers as obtained experimentally. This procedure is used to calculate the experimental populations in the case of vinyldichlorosilane where the basis set predicts the wrong conformer to be the more stable one.

Vibrational Frequencies and Normal Coordinate Analyses

For the assignment of the vibrational lines, we performed also the vibrational analysis for our chosen examples on DFT level to see whether or not the 6-311++G** basis set could be used for the calculation of more or less reliable vibrational spectra. Vinylmonohalo and vinyldihalo compounds have C_1 symmetry in their *gauche* forms, and C_s symmetry in their *cis* forms. Thus in *cis* the 21 vibrational modes span the irreducible representations 14 A′ and 7 A″, while they are all of A symmetry in *gauche*. The A′ modes should be polarized while the A″ modes be depolarized in the Raman spectra of the liquid pure *cis* compounds. Normal coordinate analyses were carried out for the molecules as described previously[8] to provide a complete assignment of the fundamental vibrational frequencies. An overcomplete set of internal coordinates (Table I) was used to form symmetry coordinates (Table II). Redundant internal coordinates are removed automatically by our PED program and are used only to facilitate the construction of symmetry coordinates. The formalism for that is outlined in Appendix.

DISCUSSION

Relative Energies

In Table III we list the total and relative energies of *cis* and *gauche* conformers for our series of compounds, CH_2=CH–AXY_2, A being carbon, silicon or germanium, X and Y being hydrogen, fluorine or chlorine.

The energies of the Ge compounds are from our previous paper[6] and have been added for the sake of completeness. Five experimental relative energies as found in the literature are also included. First of all we have to notice that all relative energies are very small, mostly just about 0.5 kcal/mol, only in a few cases 1.5 kcal/mol are reached. With such small energy differences it is not surprising that calculations on DFT or MP2 level are not too reliable, even experimental determinations of the stable conformers are sometimes not very reliable within expected experimental errors.

However, note that with the exception of some of the Ge compounds, the calculated predictions of most stable conformers are all in line with arguments based on steric effects alone. These steric effects tell that in monohalo compounds (X = halogen, Y = H), *cis* forms should be less stable than *gauche* ones, because in *cis* the bigger halogen atom eclipses the C=C double bond, experiencing higher steric hindrance than in *gauche* where a

TABLE I
Internal coordinate definitions (see Fig. 1 for atom denotation) for our series of molecules $H_2C{=}CH{-}AXY_2$ where A is C, Si, and Ge, while X and Y are H or a halogen

No.	Coordinate	Definition	
1	A_1C_3	stretch	Q
2	A_1X_2	stretch	X_1
3	A_1Y_4	stretch	X_2
4	A_1Y_5	stretch	X_3
5	C_3C_6	stretch	R
6	C_3C_7	stretch	S
7	C_6H_8	stretch	P_1
8	C_6H_9	stretch	P_2
9	$C_3A_1X_2$	bend	π_1
10	$C_3A_1Y_4$	bend	π_2
11	$C_3A_1Y_5$	bend	π_3
12	$X_2A_1Y_4$	bend	ε_1
13	$X_2A_1Y_5$	bend	ε_2
14	$Y_4A_1Y_5$	bend	ε_3
15	$C_6C_3A_1$	bend	β_1
16	$A_1C_3H_7$	bend	β_2
17	$C_6C_3H_7$	bend	β_3
18	$H_8C_6H_9$	bend	α_1
19	$C_3C_6H_8$	bend	α_2
20	$C_3C_6H_9$	bend	α_3
21	$H_7C_3C_6A_1$	wag	ω
22	$H_8C_6C_3A_1 - H_9C_6C_3A_1$	torsion	ξ_1
23	$H_8C_6C_3A_1 + H_9C_6C_3A_1$	torsion	ξ_2
24	$X_2A_1C_3C_6 + Y_4A_1C_3C_6 + Y_5A_1C_3C_6$	torsion	τ

TABLE II

Symmetry coordinates for our series of molecules, $H_2C{=}CH{-}AXY_2$ where A is C, Si, and Ge, while X and Y are H or a halogen. Coordinates are not normalized

Species	Description		Coordinate
A′	C–H	stretch	$S_1 = S$
	CH_2	antisymmetric stretch	$S_2 = P_1 - P_2$
	CH_2	symmetric stretch	$S_3 = P_1 + P_2$
	AX	stretch	$S_4 = X_1$
	AY_2	symmetric stretch	$S_5 = X_2 + X_3$
	CA	stretch	$S_6 = Q$
	CC	stretch	$S_7 = R$
	CH_2	deformation (scissor)	$S_8 = 2\alpha_1 - \alpha_2 - \alpha_3$
	CH_2	wag	$S_9 = \alpha_2 - \alpha_3$
	AX	deformation	$S_{10} = \varepsilon_1 + \varepsilon_2 - 2\varepsilon_3$
	AY_2	deformation	$S_{11} = \varepsilon_1 + \varepsilon_2 + \varepsilon_3 - \pi_1 - \pi_2 - \pi_3$
	AY_2	deformation	$S_{12} = 2\pi_1 - \pi_2 - \pi_3$
	CCA	bend	$S_{13} = 2\beta_1 - \beta_2 - \beta_3$
	CH	bend (in-plane)	$S_{14} = \beta_2 - \beta_3$
A″	AY_2	antisymmetric stretch	$S_{15} = X_2 - X_3$
	CH	bend (out-of-plane)	$S_{16} = \omega$
	CH_2	deformation I	$S_{17} = \xi_1$
	CH_2	deformation II	$S_{18} = \xi_2$
	AX	deformation	$S_{19} = \pi_2 - \pi_3$
	AY_2	deformation	$S_{20} = \varepsilon_1 - \varepsilon_2$
	AXY_2	torsion	$S_{21} = \tau$

TABLE III

Total energies, E_t (in hartrees), and relative energies, E_r (in cal mol^{-1}), for the *cis* and *gauche* conformers of vinylhalomethanes (H_2C=CH–AXY_2, A = C), vinylhalosilanes (H_2C=CH–AXY_2, A = Si) and, for the sake of completeness, for vinylhalogermanes (H_2C=CH–AXY_2, A = Ge)[6], as calculated by DFT and MP2, using a 6-311++G** atomic basis set

Y	Method	Conformer	E_t	E_r
		Monofluoro derivatives (X = F, Y = H)		
C	DFT	*cis*	–217.2087946	54
C	DFT	*gauche*	–217.2088810	0
C	MP2	*cis*	–216.6193601	336
C	MP2	*gauche*	–216.6198948	0
C	exp[14]	*gauche*		166–752
Si	DFT	*cis*	–468.6742356	390
Si	DFT	*gauche*	–468.6748568	0
Si	MP2	*cis*	–467.7028304	558
Si	MP2	*gauche*	–467.7037197	0
Ge	DFT	*cis*	–2256.1367067	128
Ge	DFT	*gauche*	–2256.1369102	0
Ge	MP2	*cis*	–2254.0551013	246
Ge	MP2	*gauche*	–2254.0554935	0
		Difluoro derivatives (X = H, Y = F)		
C	DFT	*cis*	–316.4865476	0
C	DFT	*gauche*	–316.4853600	745
C	MP2	*cis*	–314.8750530	0
C	MP2	*gauche*	–314.8742956	475
C	exp[32]	*gauche*		234 ± 2
Si	DFT	*cis*	–568.0189718	0
Si	DFT	*gauche*	–568.0185988	234
Si	MP2	*cis*	–566.8626258	0
Si	MP2	*gauche*	–566.8622981	206
Si	exp[33]	*gauche*		339 ± 33
Ge	DFT	*cis*	–2355.4541242	64
Ge	DFT	*gauche*	–2355.4542268	0
Ge	MP2	*cis*	–2353.1873135	72
Ge	MP2	*gauche*	–2353.1874274	0

TABLE III
(*Continued*)

Y	Method	Conformer	E_t	E_r
		Monochloro derivatives (X = Cl, Y = H)		
C	DFT	*cis*	–577.5655145	1161
C	DFT	*gauche*	–577.5673642	0
C	MP2	*cis*	–576.6003338	1327
C	MP2	*gauche*	–576.6024478	0
Si	DFT	*cis*	–829.0152890	355
Si	DFT	*gauche*	–829.0158549	0
Si	MP2	*cis*	–827.6618088	449
Si	MP2	*gauche*	–827.6625250	0
Si	exp[34]	*cis*		134–346
Ge	DFT	*cis*	–2616.4960249	258
Ge	DFT	*gauche*	–2616.4964364	0
Ge	MP2	*cis*	–2614.0355382	7
Ge	MP2	*gauche*	–2614.0355501	0
		Dichloro derivatives (X = H, Y = Cl)		
C	DFT	*cis*	–1037.1850352	0
C	DFT	*gauche*	–1037.1826768	1480
C	MP2	*cis*	–1034.9473408	0
C	MP2	*gauche*	–1034.9449238	1517
Si	DFT	*cis*	–1288.6940314	0
Si	DFT	*gauche*	–1288.6936555	236
Si	MP2	*cis*	–1286.7741567	0
Si	MP2	*gauche*	–1286.7738306	205
Si	exp[11]	*cis*		111
Ge	DFT	*cis*	–3076.1691743	0
Ge	DFT	*gauche*	–3076.1691687	4
Ge	MP2	*cis*	–3073.1435169	190
Ge	MP2	*gauche*	–3073.1438190	0

smaller H atom eclipses the double bond. On the contrary, in the dihalo derivatives (X = H, Y = halogen), *gauche* should be less stable than *cis*, because when the AXY_2 rotor is in this position one of the bigger halogen atoms eclipses the C=C double bond. Thus here in *gauche* there is sterical crowding between a halogen atom and the double bond, while in *cis* the smaller hydrogen atom eclipses the double bond.

In the five experimental cases as found in the literature, two of them disagree with the argument based on steric effects only and thus with our calculations, while three agree. In the case of vinylmonofluoromethane there might be an additional electrostatic attraction between H and F atoms in the *cis* form which could overcome the steric effects and bring about the experimental preference of the *cis* form. The charges are –0.24 e on F and +0.18 e on H, while the distance between the F atom and the hydrogen at the double bond is only 2.45 Å (the values are from the MP2/6-311++G** calculations). This might give an additional stabilization to *cis*, probably not too well reproduced in the calculations. However, in the other case where the calculations have gone wrong (vinyldichlorosilane), there are no obvious reasons for the theoretical overestimation of the stability of *cis*. One should, however, view this failure of theory as not too serious, because in this system *gauche* is by only 111 cal/mol more stable than *cis*, while the theoretical stabilization of *cis* is only around 200 cal/mol. One cannot expect that MP2 or DFT can easily reproduce such very small energy differences.

Thus it seems that the basis set effect found by Galabov et al.[14] in the case of vinylmonofluoromethane is not such a serious shortcoming of the basis set at all.

Vibrational Spectra and Assignment

We have chosen three of the five experimentally known cases to calculate vibrational spectra at DFT level; two of them, vinyldifluoromethane and vinyldifluorosilane, are those where the correct most stable conformer was predicted, the other one, vinyldichlorosilane, is one where predictions were wrong. The spectra have been calculated and plotted, and the potential energy distribution (PED) among the symmetry coordinates was computed as given in the second part of Appendix. The abundances of the conformers in the conformational equilibrium were calculated on the basis of their Gibbs energies as described above in the two former cases, while in the latter case spectra were plotted using abundances from experimental energies as well

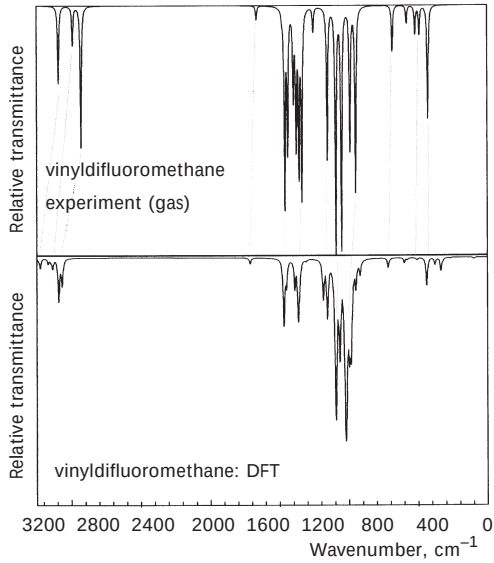

FIG. 2
Infrared spectra of vinyldifluoromethane, upper panel: experimental spectrum (gas) as replotted from ref.[32] and lower panel: theoretical spectrum obtained from our DFT calculation

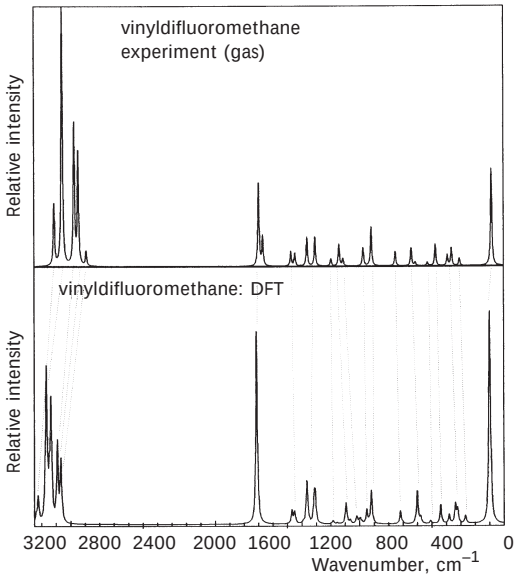

FIG. 3
Raman spectra of vinyldifluoromethane, upper panel: experimental spectrum (gas) as replotted from ref.[32] and lower panel: theoretical spectrum obtained from our DFT calculation

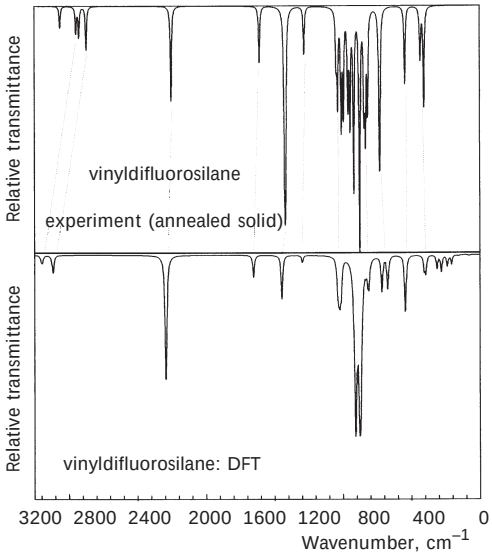

FIG. 4
Infrared spectra of vinyldifluorosilane, upper panel: experimental spectrum (annealed solid) as replotted from ref.[33] and lower panel: theoretical spectrum obtained from our DFT calculation

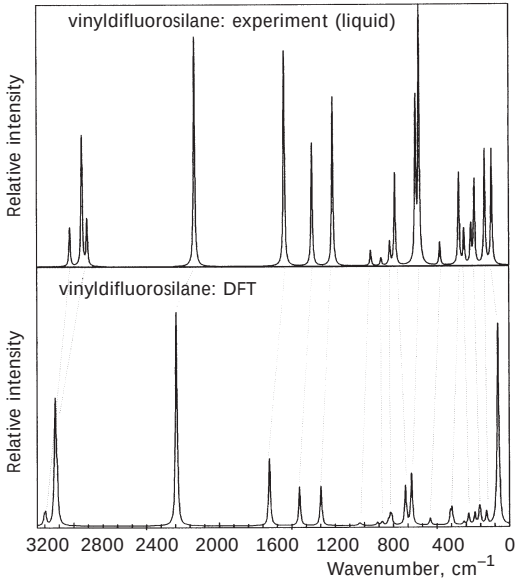

FIG. 5
Raman spectra of vinyldifluorosilane, upper panel: experimental spectrum (liquid) as replotted from ref.[33] and lower panel: theoretical spectrum obtained from our DFT calculation

as those from Gibbs energies. The calculated infrared and Raman spectra, together with the replotted experimental ones are shown in Figs 2 to 7.

Interestingly, the theoretical and experimental spectra compare rather well with each other, there is a near one-to-one correspondence between lines in the experimental and in theoretical spectra. Especially important is that this holds also in the case of vinyldichlorosilane, despite the wrongly predicted relative energies. Actually, the agreement seems to be better when experimental relative energies are used instead of theoretical Gibbs energies. However, the improvement does not go too far, because, due to the degeneracy of the *gauche* form on the potential curve for the torsion, the populations do not differ too much and *gauche* is in both cases the more

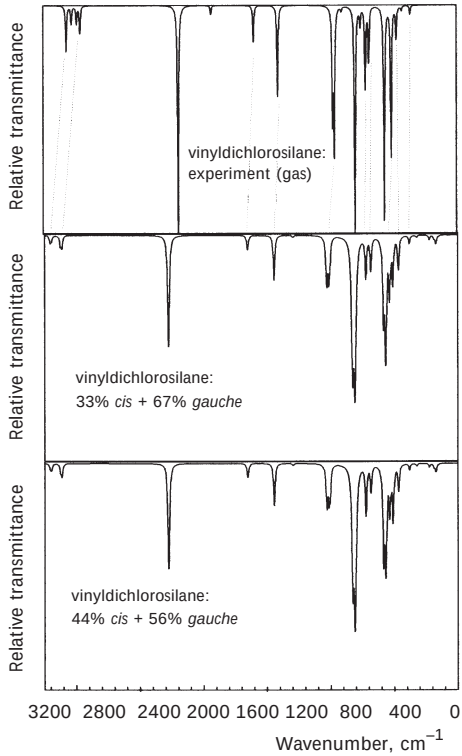

FIG. 6

Infrared spectra of vinyldichlorosilane, upper panel: experimental spectrum (gas) as replotted from ref.[11], central panel: spectra of the conformers from our DFT calculations (33% *cis* + 67% *gauche*) but with experimental[11] relative energies in a Boltzmann distribution to calculate the abundances at 298.15 K, and lower panel: completely theoretical spectrum obtained from our DFT calculation (44% *cis* + 56% *gauche*)

abundant conformer (67% from experimental energies, 56% from Gibbs energies). Note that in the latter case only the torsional mode comes out considerably too low in wavenumber in the theoretical spectra. As usual, in all spectra CH stretches appear too high in wavenumbers in theory, while the skeletal modes are usually reproduced approximately correct.

In Tables IV–VI we give the PED and the spectra for the *cis* and *gauche* conformers for our three systems.

The observed wavenumbers in comparison with the calculated ones together with the error percentages indicate the overall correctness of the theoretical spectra. The PED values are given to facilitate the assignment of the vibrational bands to individual movements within the molecules. Interest-

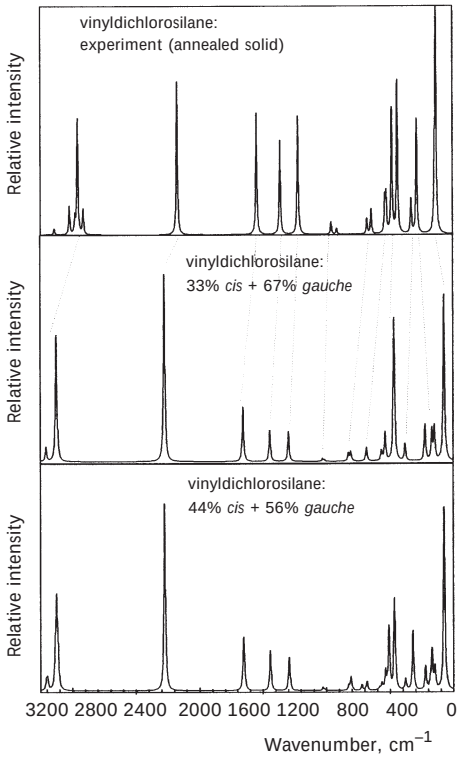

FIG. 7

Raman spectra of vinyldichlorosilane, upper panel: experimental spectrum (annealed solid) as replotted from ref.[11], central panel: spectra of the conformers from our DFT calculations (33% *cis* + 67% *gauche*) but with experimental[11] relative energies in a Boltzmann distribution to calculate the abundances at 298.15 K, and lower panel: completely theoretical spectrum obtained from our DFT calculation (44% *cis* + 56% *gauche*)

TABLE IV

Symmetry species, s_i, DFT wavenumbers, k_i (in cm^{-1}), observed wavenumbers from the literature[32], k_i(obs) (in cm^{-1}), error percentage in the DFT values, e (in %), infrared intensities, I_i (in km mol^{-1}), Raman activities, S_i (in $Å^4$ amu^{-1}), depolarization ratios ρ_i and distribution of the potential energy of a normal mode in the symmetry coordinates, PED (only values larger than 10% are given), for the normal modes i in *cis*- and *gauche*-vinyldifluoromethane (CH_2=CH–CF_2H)

s_i	k_i	k_i(obs)	e	I_i	S_i	ρ_i	PED
				cis-Vinyldifluoromethane			
A″	97	93	4.3	0.45	4.02	0.75	100% S_{21}
A″	322	323	0.3	1.14	2.54	0.75	74% S_{19}, 14% S_{18}, 11% S_{16}
A′	336	338	0.6	7.64	1.83	0.54	74% S_{13}, 19% S_{12}
A′	439	444	1.1	17.19	2.25	0.48	28% S_{11}, 28% S_{10}, 25% S_{12}, 15% S_6
A′	600	606	1.0	3.00	2.70	0.13	44% S_{11}, 23% S_5, 11% S_{12}, 10% S_6
A″	702	683	2.8	0.53	0.58	0.75	58% S_{18}, 18% S_{19}, 13% S_{16}, 11% S_{15}
A′	919	911	0.9	8.20	4.28	0.09	51% S_9, 21% S_6
A″	984	948	3.8	48.85	0.94	0.75	96% S_{17}
A″	1017	1006	1.1	59.60	2.74	0.75	78% S_{16}, 12% S_{18}
A″	1023	1061	3.6	218.17	2.94	0.75	85% S_{15}, 12% S_{18}
A′	1094	1105	1.0	181.00	5.88	0.35	66% S_5, 16% S_{10}
A′	1184	1176	0.7	24.48	3.01	0.72	35% S_{18}, 20% S_9, 17% S_{14}, 16% S_{12}, 10% S_{13}
A′	1307	1283	1.9	1.12	6.74	0.26	58% S_{14}, 18% S_9
A″	1355	1347	0.6	11.47	4.22	0.75	98% S_{20}
A′	1365	1354	0.8	27.85	13.86	0.34	55% S_{11}, 15% S_8, 12% S_{12}, 11% S_7
A′	1468	1439	2.0	46.32	7.27	0.47	70% S_8, 11% S_{11}
A′	1712	1662	3.0	2.83	35.11	0.07	71% S_7, 13% S_8
A′	3090	2966	4.2	27.62	74.03	0.22	99% S_4
A′	3135	3006	4.3	5.77	90.99	0.13	96% S_3
A′	3167	3054	3.7	1.68	97.89	0.29	96% S_1
A′	3224	3104	3.9	6.02	60.67	0.57	95% S_2

TABLE IV
(*Continued*)

s_i	k_i	k_i(obs)	e	I_i	S_i	ρ_i	PED
				gauche-Vinyldifluoromethane			
A	100	98	2.0	0.59	3.77	0.75	100% S_{21}
A	267	274	2.6	0.52	1.26	0.59	48% S_{13}, 44% S_{19}
A	379	383	1.0	8.16	2.76	0.63	31% S_{12}, 19% S_{19}, 14% S_{18}
A	508	518	1.9	2.62	1.51	0.64	64% S_{10}, 12% S_{11}
A	578	566	2.1	2.40	2.89	0.57	23% S_{13}, 22% S_{19}, 20% S_{18}
A	717	712	0.7	11.83	3.04	0.18	23% S_{18}, 21% S_5, 20% S_6
A	950	946	0.4	31.44	3.39	0.03	36% S_6, 29% S_{12}, 14% S_{18}
A	988	956	3.3	49.48	1.37	0.75	99% S_{17}
A	1019	1023	0.4	32.14	1.62	0.54	77% S_{16}, 19% S_{18}
A	1065	1089	2.2	145.19	2.87	0.49	38% S_5, 21% S_{15}, 19% S_9
A	1154	1156	0.2	79.96	1.45	0.61	25% S_5, 16% S_6, 13% S_9, 12% S_{15}, 11% S_{10}
A	1314	1288	2.0	0.66	15.93	0.29	58% S_{14}, 14% S_9, 13% S_7
A	1363	1347	1.2	25.56	4.23	0.55	62% S_{20}, 23% S_{11}
A	1390	1376	1.0	36.93	4.99	0.73	38% S_{11}, 32% S_{20}, 15% S_{12}
A	1449	1421	2.0	32.09	11.60	0.43	77% S_8
A	1712	1662	3.0	1.38	38.05	0.07	71% S_7, 12% S_8
A	3066	2952	3.9	34.29	119.95	0.23	100% S_4
A	3147	2995	5.1	3.55	62.88	0.17	91% S_3
A	3167	3044	4.0	3.05	131.94	0.21	90% S_1
A	3237	3108	4.2	2.67	51.50	0.70	99% S_2

TABLE V

Symmetry species, s_i, DFT wavenumbers, k_i (in cm^{-1}), observed wavenumbers from the literature[33], k_i(obs) (in cm^{-1}), error percentage in the DFT values, e (in %), infrared intensities, I_i (in km mol^{-1}), Raman activities, S_i (in $Å^4$ amu^{-1}), depolarization ratios ρ_i and distribution of the potential energy of a normal mode in the symmetry coordinates, PED (only values larger than 10% are given), for the normal modes i in *cis*- and *gauche*-vinyldifluorosilane (CH_2=CH–SiF_2H)

s_i	k_i	k_i(obs)	e	I_i	S_i	ρ_i	PED
				cis-Vinyldifluorosilane			
A″	76	70	8.6	0.22	4.83	0.75	100% S_{21}
A″	201	200	0.5	0.20	2.69	0.75	83% S_{19}
A′	207	220	5.9	11.42	1.58	0.51	58% S_{13}, 37% S_{12}
A′	281	295	4.7	20.94	2.27	0.54	50% S_{10}, 26% S_{11}, 13% S_{12}
A′	396	404	2.0	22.26	2.97	0.29	40% S_{10}, 22% S_{13}, 17% S_{12}, 13% S_6
A″	544	541	0.6	17.53	0.92	0.75	63% S_{18}, 23% S_{16}, 14% S_{19}
A′	716	724	1.1	48.02	9.11	0.02	63% S_6
A′	820	831	1.3	21.64	5.22	0.57	46% S_5, 31% S_{11}, 12% S_{12}
A″	821	842	2.5	2.88	7.88	0.75	75% S_{20}, 25% S_{15}
A′	873	892	2.1	346.00	2.49	0.60	41% S_5, 36% S_{11}, 10% S_6
A″	908	950	4.4	264.76	1.78	0.75	74% S_{15}, 21% S_{20}
A″	1014	968	4.8	42.42	0.68	0.75	100% S_{17}
A′	1029	1008	2.1	12.33	2.22	0.69	61% S_9, 30% S_{14}
A″	1040	1022	1.8	16.72	0.08	0.75	71% S_{16}, 29% S_{18}
A′	1296	1277	1.5	6.25	11.22	0.17	60% S_{14}, 26% S_9
A′	1447	1421	1.8	30.17	19.47	0.35	73% S_8, 20% S_7
A′	1653	1606	2.9	12.26	21.24	0.05	68% S_7, 26% S_8
A′	2293	2234	2.6	94.45	111.08	0.14	100% S_4
A′	3113	2968	4.9	11.02	79.87	0.14	96% S_3
A′	3130	3011	4.0	0.58	146.34	0.28	94% S_1
A′	3193	3073	3.9	8.41	75.22	0.58	97% S_2

TABLE V
(*Continued*)

s_i	k_i	k_i(obs)	e	I_i	S_i	ρ_i	PED
				gauche-Vinyldifluorosilane			
A	79	79	0.0	0.48	4.66	0.75	100% S_{21}
A	158	175	9.7	0.92	1.12	0.62	55% S_{19}, 39% S_{13}
A	238	248	4.0	11.72	2.57	0.69	39% S_{12}, 16% S_{11}, 15% S_{19}
A	313	327	4.3	14.48	1.05	0.69	73% S_{10}
A	408	430	5.1	15.21	3.52	0.52	38% S_{13}, 20% S_{19}, 17% S_{12}
A	546	535	2.1	54.54	2.47	0.51	48% S_{18}, 16% S_{16}, 12% S_{11}
A	674	684	1.5	37.54	10.00	0.06	68% S_6
A	811	824	1.6	26.80	6.33	0.56	48% S_5, 19% S_{20}, 18% S_{11}
A	834	847	1.5	7.94	7.56	0.74	58% S_{20}, 19% S_{15}, 14% S_5
A	880	896	1.8	316.26	3.88	0.73	39% S_{11}, 27% S_5, 14% S_{12}, 10% S_6
A	909	948	4.1	236.31	2.91	0.70	74% S_{15}, 18% S_{20}
A	1022	978	4.5	36.94	0.86	0.63	100% S_{17}
A	1031	1010	2.1	23.78	1.26	0.62	58% S_9, 28% S_{14}
A	1039	1022	1.7	18.24	0.52	0.48	70% S_{16}, 28% S_{18}
A	1299	1272	2.1	2.65	13.27	0.15	60% S_{14}, 25% S_9
A	1445	1413	2.3	26.54	19.49	0.32	75% S_8, 17% S_7
A	1652	1611	2.5	14.38	22.95	0.05	70% S_7, 24% S_8
A	2293	2236	2.5	119.61	164.45	0.17	100% S_4
A	3116	–	–	9.58	43.03	0.64	50% S_3, 49% S_1
A	3125	–	–	4.18	183.42	0.16	50% S_3, 49% S_1
A	3202	–	–	5.71	67.53	0.68	99% S_2

TABLE VI

Symmetry species, s_i, DFT wavenumbers, k_i (in cm^{-1}), observed wavenumbers from the literature[11], k_i(obs) (in cm^{-1}), error percentage in the DFT values, e (in %), infrared intensities, I_i (in km mol^{-1}), Raman activities, S_i (in $Å^4$ amu^{-1}), depolarization ratios ρ_i and distribution of the potential energy of a normal mode in the symmetry coordinates, PED (only values larger than 10% are given), for the normal modes i in *cis*- and *gauche*-vinyldichlorosilane (CH_2=CH–$SiCl_2H$)

s_i	k_i	k_i(obs)	e	I_i	S_i	ρ_i	PED
				cis-Vinyldichlorosilane			
A″	76	103	26.2	0.00	5.49	0.75	92% S_{21}
A″	172	175	1.7	0.09	3.35	0.75	80% S_{19}
A′	173	175	1.1	6.38	2.67	0.73	39% S_{11}, 30% S_{10}, 27% S_{12}
A′	186	189	1.6	4.14	1.79	0.70	42% S_{10}, 34% S_{13}, 23% S_{12}
A′	321	322	0.3	2.84	8.24	0.18	40% S_{13}, 19% S_5, 12% S_{10}, 12% S_6
A′	509	505	0.8	60.45	12.68	0.05	77% S_5, 10% S_{13}
A″	512	531	3.6	20.15	1.50	0.75	56% S_{15}, 32% S_{18}, 12% S_{16}
A″	583	589	1.0	158.36	3.91	0.75	43% S_{15}, 36% S_{18}, 11% S_{16}
A′	722	730	1.1	68.79	2.56	0.21	80% S_6
A″	809	810	0.1	156.44	9.46	0.75	95% S_{20}
A′	809	810	0.1	149.65	6.76	0.69	50% S_{11}, 36% S_{12}
A″	1004	973	3.2	36.02	0.62	0.75	100% S_{17}
A′	1029	997	3.2	10.37	2.73	0.57	62% S_9, 29% S_{14}
A″	1037	1004	3.3	15.41	0.02	0.75	73% S_{16}, 27% S_{18}
A′	1291	1272	1.5	0.88	15.07	0.16	61% S_{14}, 25% S_9
A′	1442	1407	2.5	25.46	28.42	0.34	74% S_8, 19% S_7
A′	1648	1603	2.8	10.50	28.19	0.09	69% S_7, 25% S_8
A′	2275	2219	2.5	71.61	125.43	0.15	100% S_4
A′	3115	2965	5.1	10.34	102.58	0.15	96% S_3
A′	3135	3030	3.5	0.38	123.93	0.28	94% S_1
A′	3195	3074	3.9	7.39	95.47	0.57	97% S_2

TABLE VI
(*Continued*)

s_i	k_i	k_i(obs)	e	I_i	S_i	ρ_i	PED
				gauche-Vinyldichlorosilane			
A	73	103	29.1	0.19	4.57	0.75	100% S_{21}
A	148	156	5.1	0.39	2.26	0.65	71% S_{19}, 21% S_{13}
A	168	175	4.0	3.88	3.79	0.75	40% S_{10}, 36% S_{11}, 17% S_{12}
A	222	226	1.8	3.28	2.69	0.45	40% S_{10}, 28% S_{12}
A	379	371	2.2	5.84	3.45	0.53	58% S_{13}
A	465	482	3.5	26.40	12.64	0.03	74%S_5, 11% S_{18}
A	536	536	0.0	51.02	5.86	0.34	37% S_{18}, 21% S_{15}, 14% S_{16}, 12% S_5
A	566	589	3.9	150.02	5.05	0.64	69% S_{15}, 13% S_{18}
A	683	694	1.6	27.10	4.00	0.35	71% S_6
A	807	810	0.4	142.64	8.49	0.68	67% S_{20}, 11% S_{11}
A	825	824	0.1	197.73	9.59	0.75	31% S_{11}, 29% S_{12}, 27% S_{20}
A	1013	977	3.7	32.69	0.85	0.43	100% S_{17}
A	1027	997	3.0	14.53	2.05	0.60	62% S_9, 29% S_{14}
A	1028	1004	2.4	16.98	0.17	0.24	70% S_{16}, 28% S_{18}
A	1296	1272	1.9	1.14	12.19	0.13	63% S_{14}, 25% S_9
A	1443	1413	2.1	24.86	23.26	0.35	76% S_8, 19% S_7
A	1653	1603	3.1	7.57	27.41	0.08	70% S_2, 23% S_8
A	2275	2218	2.6	87.52	177.94	0.17	100% S_4
A	3111	2965	4.9	4.72	66.28	0.65	82% S_1, 17% S_3
A	3125	3001	4.1	7.18	185.26	0.13	83% S_1, 17% S_1
A	3205	3079	4.1	4.89	73.96	0.62	99% S_2

ingly, in the molecules where the relative stabilities of the conformers were predicted wrongly, the theory severly underestimates the wavenumbers of the torsional modes by as much as about 30%, while in all other modes the largest occurring errors are usually about 5%, going up to about 9%, again for the torsional mode. Unexpectedly large errors (30%) in the torsional wavenumbers might be indicative for failures in the relative energy predictions, because the other system, vinylmonofluoromethane, appears to exhibit also a rather large torsional wavenumber[35]. Assignments on the basis of the calculated PED are rather straightforward for modes of lower wavenumbers, as well as for stretches on the upper end of the spectra, while the skeletal modes around the centers of the spectra appear to be considerably mixed.

CONCLUSION

Our final conclusion is that the shortcomings of the 6-311++G** basis set reported by Galabov et al.[14] on vinylmonofluoromethane are not very general at all. It seems they show up mainly in that specific system because of some polar effects in addition to the expected steric ones. In the other system where the basis set makes a wrong prediction this seems to be due just to the very small energy differences, which cannot be expected to be accurately described by medium-size basis sets and comparatively low-level computational methods and thus are not due to any inbalance in the basis set. Vibrational spectra were well reproduced by our DFT/6-311++G** calculations, even in the case where relative energies of conformers were predicted wrongly. Thus further use of this kind of basis set seems to be possible without big problems; however, large errors in torsional wavenumbers seem to be indicative of accompanying errors in relative energy predictions. We currently plan to report in a forthcoming publication a similar investigation using the corresponding basis set without diffuse functions to see whether in our basis set it is really the addition of diffuse functions that can be the cause of problems.

APPENDIX

Calculation of Vibrational Infrared and Raman Spectra

For calculation of the Raman spectra we used the scattering activities S_j, the wavenumbers k_j and the depolarization ratios ρ_j for each normal mode j as

calculated by the program Gaussian98 [5]. Then the Raman cross-sections which are proportional to the intensities are given as[10,36]

$$\frac{\partial\sigma_j}{\partial\Omega} = \frac{2^4\pi^4}{45}\frac{h\left(k_o - k_j\right)^4}{8\pi^2 c k_j[1-\mathrm{e}^{-\frac{hck_j}{k_B T}}]} S_j \frac{1-\rho_j}{1+\rho_j} . \qquad (A1)$$

Since we are interested only in relative intensities, we calculated them as

$$I_j = \frac{\partial\sigma_j}{\partial\Omega} \Big/ \frac{\partial\sigma_{j_m}}{\partial\Omega} \qquad (A2)$$

where j_m denotes the line among all the lines from all conformers present in the mixture that has the largest Raman cross-section. As laser wavelength we used that of an argon ion laser at λ_o = 514.5 nm ($k_o = 1/\lambda_o$). As temperature we used T = 298.15 K. Then the line shapes are calculated as Lorentzians (L) with a width of Δk = 10 cm^{-1} corresponding to the estimated average width in the experimental spectra used for comparison. Thus the final spectrum for one conformer of a molecule is calculated as

$$I'(k) = \sum_j I_j L(k-k_j); \; I(k) = \frac{I'(k)}{I_m}; \; I_m = \max\{I'(k)\}$$

$$L(k-k_j) = \frac{1}{\pi}\frac{\Delta k/2}{(k-k_j)^2 + \left(\Delta k/2\right)^2} \qquad (A3)$$

$$\int_{-\infty}^{\infty} L(k-k_j)\,\mathrm{d}k = 1$$

where the index j runs over all normal modes. For the plots a step size for the grid of generally 10 cm^{-1} was used. However, when a line appears between two consecutive grid points, N_p extra points with a step size of $\Delta k/(N_p/2)$ are inserted (here N_p = 12 is used; note that N_p in the input should be even) into this interval which include the exact center of the line.

In our systems always more than one conformer was present. Thus after calculation of the spectra of all conformers, they are superimposed with the help of a Boltzmann distribution for free energy differences. Then the total intensity as function of wavenumber for a mixture of N + 1 different conformers is given by

$$I'(k) = \frac{\sum_{l=0}^{N} g_l I_l(k) \mathrm{e}^{-\frac{\Delta G_l^\circ}{RT}}}{\sum_{l=0}^{N} g_l \mathrm{e}^{-\frac{\Delta G_l^\circ}{RT}}} \; ; \; I(k) = \frac{I'(k)}{I_m} \; ; \; I_m = \max\{I'(k)\} . \qquad (A4)$$

Here $I_l(k)$ are the individual spectra of the conformers, $l = 0$ corresponds to the most stable conformer, ΔG_l° denotes the Gibbs energy difference between conformer l and the one chosen as 0 (see the main text for details), and g_l is the degeneracy of conformer l (in our case 2 for *gauche* conformers and 1 for *cis* ones). The renormalization ensures that relative intensities vary between 0 and 1.

The intensities given by the program for infrared (IR) spectra are calculated at all the levels of computation used. They represent actually integrated absorption coefficients A_j for the different normal modes j of a system. The Lambert–Beer law tells that at any wavenumber k of an absorption band corresponding to a normal mode j

$$\log_{10} \frac{I}{I_o} = -\varepsilon_j(k) c l \qquad (A5)$$

holds, where I is the light intensity after passing through the sample, I_o the incident intensity, $\varepsilon_j(k)$ the molar absorption coefficient for mode j at wavenumber k, c the concentration and l the optical path length. If c is given in mol cm^{-3} and l in cm, then ε must be expressed in cm^2 mol^{-1}. Calculation of the integrated absorption coefficient A_j of a line j,

$$A_j = \int_{-\infty}^{\infty} \varepsilon_j(k) \, \mathrm{d}k \qquad (A6)$$

adds a factor of cm^{-1} to the unit of $\varepsilon_j(k)$ and thus A_j has the unit cm mol^{-1}. However, for a transmittance $T = I/I_o$ of 0.1 in a line of width 0, a concentration of 0.1 mol l^{-1} and a path length of 1 cm, an integrated absorption coefficient A_j of the order 10 000 cm mol^{-1} would be needed, and even larger than that if $T = 0.1$ is for the peak transmittance of a line with finite width. Thus the program gives A_j in units of km mol^{-1}, and therefore in this case $A_j = 0.1$ km mol^{-1}. Thus in the case of IR lines a Lorentzian shape is given to $\varepsilon_j(k)$

$$\varepsilon_j(k) = \frac{A_j}{\pi} \frac{\Delta k / 2}{(k - k_j)^2 + (\Delta k / 2)^2} \qquad (A7)$$

where k_j is the band center and Δk the line width as above. Note, that the Lorentzian gives the $\varepsilon_j(k)$-s the correct unit. Then the spectral absorption coefficient for a molecule is calculated as

$$\varepsilon(k) = \sum_j \varepsilon_j(k) = \sum_j \frac{A_j}{\pi} \frac{\Delta k / 2}{(k - k_j)^2 + (\Delta k / 2)^2} . \qquad (A8)$$

If there is only one conformer present the relative transmittance at each wavenumber is calculated as

$$T(k) = 10^{-\varepsilon(k)/\varepsilon_m}$$

$$\varepsilon_m = \max\{\varepsilon(k)\} . \qquad (A9)$$

Thus ε_m represents $1/(cl)$. A mixture of more than one molecule is treated similarly as in the case of Raman spectra with the help of populations P_l of conformer l

$$P_l = \frac{g_l \, \mathrm{e}^{-\frac{\Delta G_l^\circ}{RT}}}{\sum_{l=0}^{N} g_l \, \mathrm{e}^{-\frac{\Delta G_l^\circ}{RT}}} \qquad (A10)$$

with the same meaning of the symbols as in Eq. (*A4*). Thus with the spectral absorption coefficents $\varepsilon_l(k)$ for each conformer l calculated as described above, the total spectral absorption coefficient is given by

$$\varepsilon(k) = \sum_{l=0}^{N} P_l \varepsilon_l(k) = \sum_{l=0}^{N} P_l \sum_j \varepsilon_{lj}(k) \qquad (A11)$$

and finally the relative transmittance of the mixture again by Eq. (*A9*) where now ε_m represents also $1/(cl)$, however, with c being the concentration of all conformations together, and (cl) for the plot chosen such that the spectral absorption coefficent varies between 0 and 1, and thus relative transmittances between 0.1 and 1.

Potential Energy Distribution (PED) Calculation

To start our PED calculations, we read from the Gaussian output the normal mode wavenumbers k_k in cm^{-1} and the coefficients $\boldsymbol{N}_x$ in cartesian coordinates. Because we have to take some precautions due to the fact that these

coefficients are given only to an accuracy of two digits after the decimal point, we outline our procedures here[8] in some detail, although they are based on the considerations given in Wilson's book[7]. First of all, to arrive at a consistent system of units with masses in amu, lengths in ? and force constants in mdyne/Å we calculate

$$\varepsilon_k = \left(\frac{k_k}{\sqrt{f_k / m_k^*}} \right)^2 = \left(\frac{k_k}{1302.78} \right)^2 \qquad (A12)$$

where f_k is the force constant, m^*_k the effective mass and k_k the wavenumber in cm^{-1} of normal mode k, as given in the output. Note that singly underlined quantities are column vectors, while doubly underlined ones are matrices. The vector of normal coordinates is then

$$\boldsymbol{n} = \boldsymbol{N}_x^+ \boldsymbol{x} \qquad (A13)$$

where the dagger denotes (for our real matrices here) the transpose of a matrix, $\boldsymbol{x}$ is a vector containing the $3N$ (N is the number of atoms) cartesian displacements (3 for each atom) from equilibrium, $\boldsymbol{N}_x$ is thus a $3N \times (3N - 6)$ matrix, because translations and rotations are not included so far. Therefore

$$n_k = \sum_i (\boldsymbol{N}_x^+)_{ki} x_i = \sum_i (\boldsymbol{N}_x)_{ik} x_i \; . \qquad (A14)$$

As a next step because of the inaccuracies of the normal mode coefficients we normalize and orthogonalize them with respect to an "overlap" matrix $\boldsymbol{M}^{-1}$, containing the inverse atomic masses on its diagonal and 0 otherwise. Each mass has to appear three times in sequence because of the three cartesian displacements for each atom. This orthonormalization corresponds to the fact, that the mass-weighted cartesian normal mode coefficients $\boldsymbol{N}_q$ have to be orthonormal with metric $\boldsymbol{1}$

$$\boldsymbol{n} = \boldsymbol{N}_x^+ \boldsymbol{x} = \boldsymbol{N}_q^+ \boldsymbol{q} ; \quad \boldsymbol{q} = \boldsymbol{M}^{1/2} \boldsymbol{x}$$

$$\boldsymbol{N}_q = \boldsymbol{M}^{-1/2} \boldsymbol{N}_x ; \quad \boldsymbol{N}_q^+ \boldsymbol{N}_q = \boldsymbol{l} \qquad (A15)$$

$$\boldsymbol{N}_x^+ \boldsymbol{M}^{-1} \boldsymbol{N}_x = \boldsymbol{l} \; .$$

The force constant matrix $\boldsymbol{F}_q$ in mass-weighted cartesian coordinates can be derived from the fact that the potential energy V does not depend on the coordinate system

$$2V = \boldsymbol{x}^+ \boldsymbol{F}_x \boldsymbol{x} = \boldsymbol{q}^+ \boldsymbol{M}^{-1/2} \boldsymbol{F}_x \boldsymbol{M}^{-1/2} \boldsymbol{q} = \boldsymbol{q}^+ \boldsymbol{F}_q \boldsymbol{q}$$

$$\boldsymbol{F}_q = \boldsymbol{M}^{-1/2} \boldsymbol{F}_x \boldsymbol{M}^{-1/2}; \quad \boldsymbol{n} = \boldsymbol{N}_q^+ \boldsymbol{q}; \quad \boldsymbol{F}_q \boldsymbol{N}_q = \boldsymbol{N}_q \boldsymbol{\varepsilon}; \quad \varepsilon_{k'k} = \varepsilon_k \delta_{k'k}. \quad (A16)$$

Thus from our input data we can construct $\boldsymbol{F}_q$

$$\boldsymbol{F}_q = \boldsymbol{N}_q \boldsymbol{\varepsilon} \boldsymbol{N}_q^+ . \quad (A17)$$

In all further calculations we do not use the normal mode coefficients read in, but those obtained by diagonalization of the so formed $\boldsymbol{F}_q$. This yields the same eigenvalues ε_k, but somewhat more accurate coefficients $\boldsymbol{N}_q$. Note that this matrix now contains also rotations and translations and is therefore a square matrix of dimension $3N \times 3N$.

To obtain a PED, we now have to transform force constant matrices and normal mode coefficients first into a space of internal coordinates and then into one of symmetry coordinates. The latter ones define the atomic motions which one would like to assign the normal modes to, while the former ones are introduced just to make it easier to define the latter ones. For a complete description of all possible internal motions one needs at least a complete set of independent internal coordinates ($3N - 6$). Any of them can be built from the 5 primitive ones: bond stretch, bond angle bend, wag, torsion and libration. The latter ones are only needed if parts of the molecule are linear (at least 3 colinear atoms). The program input just defines what type of internal coordinate is desired together with the numbers of the atoms involved. Then following[7] and using the equilibrium geometry of the molecule which is also part of the input, the program calculates the matrix $\boldsymbol{B}$ which links the internal coordinate vector $\boldsymbol{b}$ to the cartesian displacement vector $\boldsymbol{x}$

$$\boldsymbol{b} = \boldsymbol{B}\boldsymbol{x}; \quad b_j = \sum_i B_{ji} x_i . \quad (A18)$$

The user is free to introduce an overcomplete set of internal coordinates, since this usually makes the construction of the necessary symmetry coordinates more easy. The complete set of independent internal coordinates would give a $\boldsymbol{B}$ of dimension $(3N - 6) \times 3N$, a rectangular matrix, which has no normal inverse.

The next step in the input has to provide at least $3N - 6$ coefficients which link the desired symmetry coordinate vector s to the internal coordinate vector $\boldsymbol{b}$. The coefficient matrix has to contain only orthogonal symmetry coordinates

$$\boldsymbol{s} = \boldsymbol{U}\boldsymbol{b} \,. \qquad (A19)$$

At this point there are two possibilities for the user. One can provide either a complete set of $3N - 6$ symmetry coordinates together with six orthogonal redundant coordinates, or the user can provide only the $3N - 6$ necessary orthogonal symmetry coordinates. The program detects which case is present and deals with it accordingly.

However, now as next step, redundant internal coordinates must be identified and removed from the list of internal coordinates, as well as from matrix $\boldsymbol{U}$, which links symmetry and internal coordinates. This can be done by forming a square-symmetric matrix $\boldsymbol{B}\boldsymbol{B}^+$. We use for inversions the fact that for symmetric square matrices $\boldsymbol{A}$, their inverse can be constructed from their eigenvalue $\boldsymbol{\lambda}$ (contains the eigenvalues on the diagonal and 0 else) and eigenvector matrices $\boldsymbol{V}$

$$\boldsymbol{A}^{-1} = \boldsymbol{V}\boldsymbol{\lambda}^{-1}\boldsymbol{V}^+; \;\; (\boldsymbol{\lambda}^{-1})_{j'j} = \lambda_j^{-1}\delta_{j'j} \,. \qquad (A20)$$

We first diagonalize $\boldsymbol{B}\boldsymbol{B}^+$

$$\boldsymbol{B}(\boldsymbol{B}^+)\boldsymbol{V} = \boldsymbol{V}\boldsymbol{\lambda} \,; \;\; \lambda_{j'j} = \lambda_j\delta_{j'j} \,; \;\; \boldsymbol{V}\boldsymbol{V}^+ = \boldsymbol{V}^+\boldsymbol{V} = \boldsymbol{I} \,. \qquad (A21)$$

Then we have a redundant internal coordinate for each zero eigenvalue of this matrix. The eigenvalues we can get by

$$\boldsymbol{V}^+\boldsymbol{B}\boldsymbol{B}^+\boldsymbol{V} = \boldsymbol{\lambda} \,. \qquad (A22)$$

Therefore an eigenvalue of zero with index say j_o means

$$\sum_{k'k} V_{kj_o} (\boldsymbol{BB}^+)_{k'k} V_{k'j_o} = \lambda_{j_o} = 0$$

$$\sum_{k'k} V_{kj_o} \sum_{l} B_{kl} B_{k'l} V_{k'j_o} = 0$$

$$\sum_{l} \left(\sum_{k} V_{kj_o} B_{kl} \right)^2 = 0 \qquad (A23)$$

$$\sum_{k} V_{kj_o} B_{kl} = 0 \, .$$

The excistence of a relation like the latter one between internal coordinates just proves linear dependence. To choose an internal coordinate with index k_o to be removed from the matrix $\boldsymbol{B}$, the program chooses k_o such that

$$|V_{k_o j_o}| = \max |V_{kj_o}| \, . \qquad (A24)$$

If after removal of an internal coordinate for each zero eigenvalue of $\boldsymbol{BB}^+$, there are $3N - 6$ independent coordinates left, the program goes on with the calculation. If the set is not complete, it indicates the fact in the output and stops execution. Redundants must be removed because $\boldsymbol{BB}^+$ cannot be inverted if it has zero eigenvalues.

However, now the deleted dependent coordinates have to be also removed from $\boldsymbol{U}$. Assume an internal coordinate k_o has to be removed. Then from the above dicussion we have the equation

$$B_{k_o l} = - \sum_{k \neq k_o} \frac{V_{kj_o}}{V_{k_o j_o}} B_{kl} \, . \qquad (A25)$$

Let us call the matrix still containing the redundant internal coordinate $\boldsymbol{U}'$, and the new one obtained after removal $\boldsymbol{U}$

$$s_n = \sum_k U'_{nk} b_k = \sum_k U'_{nk} = \sum_l B_{kl} x_l =$$

$$= \sum_l \left[\sum_{k \neq k_o} U'_{nk} B_{kl} + U'_{nk_o} B_{k_o l} \right] x_l = \qquad (A26)$$

$$= \sum_l \left[\sum_{k \neq k_o} U'_{nk} B_{kl} - U'_{nk_o} \sum_{k \neq k_o} \frac{V_{kj_o}}{V_{k_o j_o}} B_{kl} \right] x_l$$

In the last line of Eq. (*A26*) we just have inserted Eq. (*A25*). From this we get our new symmetry coordinate matrix as

$$s_n = \sum_{k \neq k_o} \left[U'_{nk} - \frac{V_{kj_o}}{V_{k_o j_o}} U'_{nk_o} \right] \sum_l B_{kl} x_l = \sum_{k \neq k_o} \left[U'_{nk} - \frac{V_{kj_o}}{V_{k_o j_o}} U'_{nk_o} \right] b_k$$

$$U_{nk} = U'_{nk} - \frac{V_{kj_o}}{V_{k_o j_o}} U'_{nk_o} \; ; \; k \neq k_o \; . \qquad (A27)$$

As next step the program orthogonalizes the old internal coordinates (let us call the old matrix $\boldsymbol{B}'$ from now on, and the new one $\boldsymbol{B}$) to the translations and rotations contained in $\boldsymbol{N}_q$ as obtained from diagonalization of $\boldsymbol{F}_q$. This is again necessary because of the low accuracy of the $\boldsymbol{N}_x$ input. However, corrections are small. Let us call the $6 \times 3N$ matrix, which links the translations and rotations to the cartesian displacements, $\boldsymbol{T}$. Then our new $\boldsymbol{B}$ matrix has to fulfill

$$\sum_l B_{kl} T_{jl} = 0 \qquad (A28)$$

where index j runs from 1 to 6. This is reached, by adding a linear combination of the translations and rotations with yet unknown coefficients α to the old matrix $\boldsymbol{B}'$

$$B_{kl} = B'_{kl} + \sum_{j=1}^{6} \alpha_{kj} T_{jl}$$

$$\sum_l \left[B'_{kl} + \sum_{j=1}^{6} \alpha_{kj} T_{jl} \right] T_{j'l} = 0 \; . \qquad (A29)$$

With the following definitions ($\boldsymbol{N}(T)_q$ denotes the part of $\boldsymbol{N}_q$ that describes the six translations and rotations)

$$\boldsymbol{X} \equiv \boldsymbol{T}\boldsymbol{T}^+ = \boldsymbol{N}(T)_q^+ \boldsymbol{M}^{-1} \boldsymbol{N}(T)_q$$

$$\boldsymbol{a} \equiv \boldsymbol{B}'\boldsymbol{T}^+ ; \; \boldsymbol{T} \equiv \boldsymbol{M}^{-1/2} \boldsymbol{N}(T)_q \qquad (A30)$$

we obtain

$$\boldsymbol{a} = -\boldsymbol{\alpha}\boldsymbol{X} . \qquad (A31)$$

Since $\boldsymbol{X}$ is a square but not a symmetric matrix our program cannot invert it. Thus

$$\boldsymbol{a}\boldsymbol{X}^+ = -\boldsymbol{\alpha}\boldsymbol{X}\boldsymbol{X}^+$$

$$\boldsymbol{\alpha} = -\boldsymbol{a}\boldsymbol{X}^+(\boldsymbol{X}\boldsymbol{X}^+)^{-1} . \qquad (A32)$$

Note that $\boldsymbol{X}\boldsymbol{X}^+$ is a symmetric square matrix. Thus our new $\boldsymbol{B}$ matrix is

$$\boldsymbol{B} = \boldsymbol{B}' - \boldsymbol{a}\boldsymbol{X}^+(\boldsymbol{X}\boldsymbol{X}^+)^{-1}\boldsymbol{T} . \qquad (A33)$$

Now the program adds the translations and rotations to $\boldsymbol{B}$, to get a square matrix. However, note that the procedures outlined in the following work equally well for square-unsymmetric as for rectangular matrices. If $\boldsymbol{B}$ is increased to a $3N \times 3N$ matrix, the same has to be done for the symmetry coordinate matrix $\boldsymbol{U}$. This implies simply that for each translation or rotation in $\boldsymbol{B}$ one has to add a symmetry coordinate in $\boldsymbol{U}$ which has as its only component just the internal translation or rotation coordinate under consideration.

Now we have to compute a force constant matrix in internal coordinates, $\boldsymbol{F}_b$. To this end, a look at the potential energy V again shows the way

$$2V = \boldsymbol{x}^+\boldsymbol{F}_x\boldsymbol{x} = \boldsymbol{q}^+F_q\boldsymbol{q} = \boldsymbol{n}^+\boldsymbol{\varepsilon}\boldsymbol{n} =$$

$$= \boldsymbol{b}^+\boldsymbol{F}_b\boldsymbol{b} = \boldsymbol{x}^+\boldsymbol{B}^+\boldsymbol{F}_b\boldsymbol{B}\boldsymbol{x} \qquad (A34)$$

$$\boldsymbol{F}_x = \boldsymbol{B}^+\boldsymbol{F}_b\boldsymbol{B} .$$

With $\boldsymbol{B}$ being either rectangular or not invertible with our program, we have to resort again to a trick

$$\boldsymbol{B}\boldsymbol{F}_x\boldsymbol{B}^+ = (\boldsymbol{B}\boldsymbol{B}^+)\,\boldsymbol{F}_b(\boldsymbol{B}\boldsymbol{B}^+)$$

$$\boldsymbol{F}_b = (\boldsymbol{B}\boldsymbol{B}^+)^{-1}\,\boldsymbol{B}\boldsymbol{F}_x\boldsymbol{B}^+\,(\boldsymbol{B}\boldsymbol{B}^+)^{-1} \equiv \boldsymbol{A}\boldsymbol{F}_x\boldsymbol{A}^+ \qquad (A35)$$

$$\boldsymbol{A} \equiv (\boldsymbol{B}\boldsymbol{B}^+)^{-1}\,\boldsymbol{B}\ .$$

In this way it is easy to calculate $\boldsymbol{F}_b$ from $\boldsymbol{F}_x$ for any form of $\boldsymbol{B}$. A similar procedure we have when transforming $\boldsymbol{F}_b$ to $\boldsymbol{F}_s$, the force constant matrix in symmetry coordinates

$$2V = \boldsymbol{s}^+\boldsymbol{F}_s\boldsymbol{s} = \boldsymbol{b}^+\boldsymbol{U}^+\boldsymbol{F}_s\boldsymbol{U}\boldsymbol{b} = \boldsymbol{b}^+\,\boldsymbol{F}_b\boldsymbol{b}$$

$$\boldsymbol{U}^+\boldsymbol{F}_s\boldsymbol{U} = \boldsymbol{F}_b\ . \qquad (A36)$$

From this we can calculate $\boldsymbol{F}_s$ from $\boldsymbol{F}_b$ in the same way as above. Note that in almost all cases we use our program, $\boldsymbol{U}$ is not a square orthogonal matrix. The latter would imply that $\boldsymbol{U}^{-1} = \boldsymbol{U}^+$. In that case we would simply have $\boldsymbol{F}_s = \boldsymbol{U}\,\boldsymbol{F}_b\,\boldsymbol{U}^+$.

Using the definitions $\boldsymbol{b} = \boldsymbol{N}_b\boldsymbol{n}$ and $\boldsymbol{s} = \boldsymbol{N}_s\boldsymbol{n}$, it is easy to show that $\boldsymbol{N}_b$ diagonalizes $\boldsymbol{F}_b$ and $\boldsymbol{N}_s$ diagonalizes $\boldsymbol{F}_s$. With Eq. (*A13*) we obtain

$$\boldsymbol{b} = \boldsymbol{N}_b\boldsymbol{n} = \boldsymbol{N}_b\boldsymbol{N}^+{}_x\boldsymbol{x}\ . \qquad (A37)$$

Since Eq. (*A18*) tells that also $\boldsymbol{b} = \boldsymbol{B}\boldsymbol{x}$ we get

$$\boldsymbol{B} = \boldsymbol{N}_b\boldsymbol{N}_x^+$$

$$\boldsymbol{B}\boldsymbol{M}^{-1}\boldsymbol{N}_x = \boldsymbol{N}_b\boldsymbol{N}_x^+\,\mathrm{N}_x = \boldsymbol{N}_b\ . \qquad (A38)$$

The last step uses Eq. (*A15*). Finally, again with Eq. (*A15*) we arrive at

$$\boldsymbol{N}_b = \boldsymbol{B}\boldsymbol{M}^{-1/2}\boldsymbol{N}_q = \boldsymbol{B}\boldsymbol{M}^{-1}\boldsymbol{N}_x\ . \qquad (A39)$$

In the same fashion we make use of Eqs (*A18*) and (*A19*), which tell us that

$$\boldsymbol{s} = \boldsymbol{N}_s\boldsymbol{n} = \boldsymbol{N}_s\boldsymbol{N}_x^+\boldsymbol{x} \qquad (A40)$$

and also

$$\boldsymbol{s} = \boldsymbol{Ub} = \boldsymbol{UBx} \; . \tag{A41}$$

Therefore, in the same way as for $\boldsymbol{N}_\mathrm{b}$ we get for $\boldsymbol{N}_\mathrm{s}$

$$\boldsymbol{N}_\mathrm{s} = \boldsymbol{UBM}^{-1/2}\boldsymbol{N}_\mathrm{q} = \boldsymbol{UBM}^{-1}\boldsymbol{N}_\mathrm{x} \; . \tag{A42}$$

Now using step by step Eq. (*A36*), then Eq. (*A34*), then Eq. (*A16*), and finally Eqs (*A15*) and (*A17*) we can write

$$\begin{aligned} \boldsymbol{N}_\mathrm{s}^+\boldsymbol{F}_\mathrm{s}\boldsymbol{N}_\mathrm{s} &= \boldsymbol{N}_\mathrm{q}^+\boldsymbol{M}^{-1/2}\boldsymbol{B}^+\boldsymbol{U}^+\boldsymbol{F}_\mathrm{s}\boldsymbol{UBM}^{-1/2}\boldsymbol{N}_\mathrm{q} = \\ &= \boldsymbol{N}_\mathrm{q}^+\boldsymbol{M}^{-1/2}\boldsymbol{B}^+\boldsymbol{F}_\mathrm{b}\boldsymbol{BM}^{-1/2}\boldsymbol{N}_\mathrm{q} = \\ &= \boldsymbol{N}_\mathrm{q}^+\boldsymbol{M}^{-1/2}\boldsymbol{F}_\mathrm{x}\boldsymbol{M}^{-1/2}\boldsymbol{N}_\mathrm{q} = \\ &= \boldsymbol{N}_\mathrm{q}^+\boldsymbol{F}_\mathrm{q}\boldsymbol{N}_\mathrm{q} = \boldsymbol{N}^+{}_\mathrm{q}\boldsymbol{N}_\mathrm{q}\boldsymbol{\varepsilon}\boldsymbol{N}_\mathrm{q}^+\boldsymbol{N}_\mathrm{q} = \boldsymbol{\varepsilon} \; . \end{aligned} \tag{A43}$$

Thus we arrive at

$$\boldsymbol{\varepsilon} = \boldsymbol{N}_\mathrm{q}^+\boldsymbol{F}_\mathrm{q}\boldsymbol{N}_\mathrm{q} = \boldsymbol{N}_\mathrm{s}^+\boldsymbol{F}_\mathrm{s}\boldsymbol{N}_\mathrm{s} \; . \tag{A44}$$

Therefore the potential energy in the normal mode j, ε_j, is

$$\begin{aligned} \varepsilon_j &= (\boldsymbol{N}_\mathrm{s}^+\boldsymbol{F}_\mathrm{s}\boldsymbol{N}_\mathrm{s})_{jj} = \sum_k (\boldsymbol{N}_\mathrm{s}^+)_{jk}(\boldsymbol{F}_\mathrm{s}\boldsymbol{N}_\mathrm{s})_{kj} = \\ &= \sum_k (\boldsymbol{N}_\mathrm{s})_{kj}(\boldsymbol{F}_\mathrm{s}\boldsymbol{N}_\mathrm{s})_{kj} \; . \end{aligned} \tag{A45}$$

Finally, the contribution of the symmetry coordinate k to the potential energy of normal mode j, ε_j, in percent, PED_{kj}, is given by

$$\mathrm{PED}_{kj} = \frac{(\boldsymbol{N}_\mathrm{s})_{kj}\sum_l (F_\mathrm{s})_{kl}(\boldsymbol{N}_\mathrm{s})_{lj}}{\varepsilon_j} 100\% \; . \tag{A46}$$

It is easy to see that the sum over all symmetry coordinates k yields 100% as required. However, due to the presence of negative coupling constants in $\boldsymbol{F}_\mathrm{s}$ and $\boldsymbol{F}_\mathrm{b}$, small negative percentages can occur due to the inaccuracies in the $\boldsymbol{N}_\mathrm{x}$ input. Further, if two coordinates are very strongly coupled, i.e. are

nearly linear-dependent, even percentages larger than 100% for one of them compensated by percentages less than 100% for the other can occur. In such a case one has to change either internal or symmetry coordinates, to reduce coupling constants.

The authors gratefully acknowledge the support of this work by the King Fahd University of Petroleum and Minerals.

REFERENCES

1. Badawi H. M., Förner W.: *J. Mol. Struct. (THEOCHEM)* **2001**, *561*, 103.
2. Badawi H. M., Förner W., Al-Saadi A. A.: *J. Mol. Struct. (THEOCHEM)* **2001**, *535*, 183.
3. Badawi H. M., Förner W.: *J. Mol. Struct. (THEOCHEM)* **2001**, *538*, 73.
4. Badawi H. M., Seddigi Z. S.: *J. Mol. Struct. (THEOCHEM)* **2001**, *546*, 231.
5. Frisch M. J., Trucks G. W., Schlegel H. B., Scuseria G. E., Robb M. A., Cheeseman J. R., Zakrzewski V. G., Montgomery J. A., Jr., Stratmann R. E., Burant J. C., Dapprich S., Millam J. M., Daniels A. D., Kudin K. N., Strain M. C., Farkas O., Tomasi J., Barone V., Cossi M., Cammi R., Mennucci B., Pomelli C., Adamo C., Clifford S., Ochterski J., Petersson G. A., Ayala P. Y., Cui Q., Morokuma K., Malick D. K, Rabuck A. D., Raghavachari K., Foresman J. B., Cioslowski J., Ortiz J. V., Baboul A. G., Stefanov B. B., Liu G., Liashenko A., Piskorz P., Komaromi I., Gomperts R., Martin R. L., Fox D. T., Keith T., Al-Laham M. A., Peng C. Y., Nanayakkara A., Gonzalez C., Challacombe M., Gill P. M. W., Johnson B. G., Chen W., Wong W., Andres J. L., Head-Gordon M., Replogle E. S., Pople J. A.: *Gaussian98*. Gaussian Inc., Pittsburgh (PA) 1998.
6. a) Förner W., Badawi H. M., Seddigi Z. S.: *Asian J. Spectrosc.* **2005**, *9*, 1; b) Förner W., Badawi H. M., Seddigi Z. S.: *Asian J. Spectrosc.* **2006**, *10*, 15.
7. Wilson E. B., Decius J. C., Cross P. C.: *Molecular Vibrations*. McGraw–Hill, New York 1955.
8. Förner W.: *Int. J. Quantum Chem.* **2004**, *99*, 533.
9. Badawi H. M., Baranovic G., Groner P., Zhen M., Durig J. R.: *Spectrochim. Acta, Part A* **1994**, *50*, 383.
10. Chantry G. W. in: *The Raman Effect* (A. Anderson, Ed.), Vol. 1, Chap. 2. Marcel Dekker, New York 1971.
11. a) Johansen T. H., Hagen K., Hassler K., Richardson A. D., Patzold U., Stolevik R.: *J. Mol. Struct.* **2000**, *550*, 257; b) Guirgis G. A., Zhen P., Durig J. R.: *Spectrochim. Acta, Part A* **2000**, *56*, 1957.
12. a) Badawi H. M., Förner W.: *J. Mol. Struct.* **2002**, *616*, 1; b) Förner W., Badawi H. M.: *J. Mol. Model.* **2001**, *7*, 288.
13. Badawi H. M., Förner W., Al-Saadi A. A.: *J. Mol. Struct. (THEOCHEM)* **2005**, *712*, 131.
14. Galabov B., Kenney J. P., Shaefer III H. F., Durig J. R.: *J. Phys. Chem. A* **2002**, *106*, 3625.
15. Durig J. R., Sullivan J. F., Guirgis G. A., Qtaitate M. A.: *J. Phys. Chem. A* **1991**, *95*, 1563.
16. Johansen T. H., Hagen K., Stolevik R., Hassler K.: *J. Phys. Chem. A* **1997**, *101*, 3580.
17. Johansen T. H., Hagen K., Hassler K., Richardson A., Patzold U., Stolevik R.: *J. Phys. Chem. A* **1997**, *101*, 9641.
18. Guirgis G. A., Shens Z., Qtaitate M. A., Durig J. R.: *J. Mol. Struct.* **1997**, *403*, 57.

19. Durig J. R., Nashed Y. E., Qtaitate M. A., Guirgis G. A.: *J. Mol. Struct.* **2000**, *525*, 191.
20. Guirgis G. A., Nashed Y. E., Durig J. R.: *Spectrochim. Acta, Part A* **2000**, *56*, 1056.
21. Durig J. R., Mohammad A. B., Attia G. M., Li Y. S., Cridock S.: *J. Phys. Chem. A* **1985**, *83*, 10.
22. Durig J. R., Geyer T. T., Groner P., Dakkouri M.: *Chem. Phys.* **1988**, *125*, 299.
23. Cridock S., Durig J. R., Mohammad A. B., Sullivan J. F., Koput J.: *J. Mol. Struct.* **1988**, *128*, 68.
24. Durig J. R., Attia G. M.: *Spectrochim. Acta, Part A* **1988**, *44*, 517.
25. Escudie J., Couret C., Ranaivonjatovo H., Satge J.: *Coord. Chem. Rev.* **1994**, *130*, 427.
26. Nowek A. J., Leszczynski J.: *J. Phys. Chem. A* **1997**, *101*, 3784.
27. Khabashesku V. N., Kudin N. K., Tamas J.: *J. Am. Chem. Soc.* **1998**, *120*, 5005.
28. Litz E. K., Kampf W. J., Banaszak Holl M.: *J. Am. Chem. Soc.* **1998**, *120*, 7484.
29. Katz M. S., Reichl A. J., Berry H. D.: *J. Am. Chem. Soc.* **1998**, *120*, 9844.
30. Durig J. R., Sullivan J. F., Attia G. M.: *Spectrochim. Acta, Part A* **1986**, *42*, 75.
31. Wang Y. S., Wu Z. H., Shi Y. T., Wang Y. J.: *Physica B (Amsterdam)* **1999**, *262*, 205.
32. Durig J. R., Yu Z., Guirgis G. A.: *J. Phys. Chem. A* **2000**, *104*, 741.
33. Durig J. R., Guirgis G. A., Zheng C., Mohamed T. A.: *Spectrochim. Acta, Part A* **2003**, *59*, 2099.
34. Guirgis G. A., Zheng C., Shen S., Durig J. R.: *J. Mol. Struct.* **2003**, *651*, 759.
35. Meakin P., Harris D. O., Hirota E.: *J. Chem. Phys.* **1969**, *51*, 3775.
36. Durig J. R., Guirgis G. A., Krutules K. A., Phan H., Stidham H. D.: *J. Raman Spectrosc.* **1994**, *25*, 221.